

Collapse and Nonlinear Instability of AdS Space with Angular Momentum

Matthew W. Choptuik,^{1,2,*} Óscar J.C. Dias,^{3,†} Jorge E. Santos,^{4,‡} and Benson Way^{1,§}

¹*Department of Physics and Astronomy, University of British Columbia,
6224 Agricultural Road, Vancouver, British Columbia V6T 1W9, Canada*

²*CIFAR Cosmology and Gravity Program, 180 Dundas Street W, Suite 1400, Toronto, Ontario M5G 1Z8, Canada*

³*STAG Research Centre and Mathematical Sciences, University of Southampton, Southampton SO17 1BJ, United Kingdom*

⁴*Department of Applied Mathematics and Theoretical Physics, University of Cambridge,
Wilberforce Road, Cambridge CB3 0WA, United Kingdom*

(Received 10 July 2017; revised manuscript received 7 August 2017; published 6 November 2017)

We present a numerical study of rotational dynamics in AdS₅ with equal angular momenta in the presence of a complex doublet scalar field. We determine that the endpoint of gravitational collapse is a Myers-Perry black hole for high energies and a hairy black hole for low energies. We investigate the time scale for collapse at low energies E , keeping the angular momenta $J \propto E$ in anti-de Sitter (AdS) length units. We find that the inclusion of angular momenta delays the collapse time, but retains a $t \sim 1/E$ scaling. We perturb and evolve rotating boson stars, and find that boson stars near AdS space appear stable, but those sufficiently far from AdS space are unstable. We find that the dynamics of the boson star instability depend on the perturbation, resulting either in collapse to a Myers-Perry black hole, or development towards a stable oscillating solution.

DOI: 10.1103/PhysRevLett.119.191104

Introduction.—Spacetimes with anti-de Sitter (AdS) boundary conditions play a central role in our understanding of gauge-gravity duality [1–4], where solutions to the Einstein equation with a negative cosmological constant are dual to states of strongly coupled field theories. This correspondence has inspired the study of gravitational physics in AdS space over the past two decades.

It is perhaps surprising that the issue of the nonlinear stability of (global) AdS space was only raised nine years after AdS/CFT was first formulated [5,6]. Dafermos and Holzegel conjectured a nonlinear instability where the reflecting boundary of AdS space allows for small but finite energy perturbations to grow and eventually collapse into a black hole. This is in stark contrast with Minkowski and de Sitter spacetimes, where nonlinear stability has long been established [7,8].

The first numerical evidence in favor of such an instability of AdS space was reported in [9]. This topic has since attracted much attention both from numerical and formal perspectives [10–64]; for reviews see [35,65–67]. Remarkably, this instability has recently been proved for the spherically symmetric and pressureless Einstein-massless-Vlasov system [62,63].

The collapse time scale is dual to the thermalization time in the field theory, and is important for characterizing and understanding this instability. For energies E much smaller than the AdS length $L = 1$, early evolution is well described by perturbation theory. However, irremovable resonances generically cause secular terms to grow, leading to a breakdown of perturbation theory at a time $t \sim 1/E$. Numerical evidence suggests that horizon formation occurs shortly thereafter, i.e., at this same time scale [9,12,13,27–29,36,42,44]. It is not fully understood why collapse seems

to occur at the shortest time scale allowed by perturbation theory, though see [52] for some recent progress.

However, all numerical studies have been restricted to zero angular momentum. Though perturbation theory breaks down at $t \sim 1/E$ for systems with rotation as well [10,53,64], this only places a lower bound on the time scale for gravitational collapse. It therefore remains unclear whether rotational forces could balance the gravitational attraction and delay the collapse time.

The inclusion of angular momentum also enriches the phase diagram of solutions. In addition to the Myers-Perry (and Kerr) family of rotating black holes, there are “black resonators” [68], which can be described as black holes with gravitational hair, and “geons” [10,35,61], which are horizonless gravitational configurations held together by their own self-gravity. The nonlinear dynamics of these solutions remain largely unexplored.

Because of the lack of symmetries, the inclusion of angular momenta poses a numerical challenge (though see [69] for recent progress away from spherical symmetry). For instance, the dynamical problem for pure gravity in four dimensions requires a full 3 + 1 simulation. To reduce numerical cost (see [24,50,59,70,71] for the use of a similar strategy), we will rely on the fact that in odd dimensions ($d \geq 5$), black holes have an enhanced symmetry when all of their angular momenta are equal. This simplification alone is insufficient for our purposes, since gravitons that carry angular momenta break these symmetries. We therefore introduce a complex scalar doublet Π given by the action

$$S = \frac{1}{16\pi G_5} \int d^5x \sqrt{-g} (R + 12 - 2|\nabla\Pi|^2). \quad (1)$$

As we shall see, this theory admits an ansatz with which one can study gravitational collapse with angular momentum using a 1 + 1 numerical simulation.

Moreover, this ansatz has a phase diagram of stationary solutions that is similar to that of pure gravity [72]. In particular, this theory contains hairy black holes and boson stars, which are somewhat analogous to black resonators and geons, respectively. Consequently, in addition to gravitational collapse, we are also able to investigate the dynamics of hairy black holes and boson stars.

Again, in this context, hairy black holes are much like black resonators, only with scalar hair instead of gravitational hair. Both the hairy black holes and boson stars exist for energies and angular momenta where Myers-Perry black holes are superextremal and singular. For these conserved quantities, the weak cosmic censorship conjecture therefore implies that the final state following gravitational collapse cannot be a Myers-Perry black hole. For evolution respecting the symmetries of our ansatz, we wish to test cosmic censorship by identifying the endpoint of collapse.

Boson stars are horizonless solutions with a stationary metric and harmonically oscillating scalar field [13,72,73]. They are important objects for the study of the AdS instability since, like geons (and oscillons [14,40] for a real scalar field), they can be generated as nonlinear extensions of normal modes of AdS space. Such solutions can avoid the resonance phenomenon that leads to perturbative breakdown. Indeed, simulations of some of these solutions indicate stability well past $t \sim 1/E$ [11,13,14,27–29,43,44]. Initial data near these solutions therefore lie within an “island of stability.” We wish to investigate whether this stability applies for rotating boson stars.

However, boson stars far from AdS space (i.e., past a turning point in their phase diagram) are expected to be unstable. We aim to determine the endpoint of this instability.

Method.—We describe our ansatz and equations of motion schematically here; a full account is given in the Supplemental Material [74], which includes Refs. [72, 75–78]. Our metric and scalar are

$$ds^2 = \frac{1}{(1-\rho^2)^2} \left\{ -\alpha^2 \left[1 - \rho^2(2-\rho^2) \frac{\beta^2}{a} \right] dt^2 + \frac{4\alpha\beta}{a} \rho dt d\rho + \frac{d\rho^2}{a(2-\rho^2)} + \rho^2(2-\rho^2) \left[\frac{1}{b^2} (d\psi + \cos^2\left(\frac{\theta}{2}\right) d\phi - \Omega dt)^2 + \frac{b}{4} (d\theta^2 + \sin^2\theta d\phi^2) \right] \right\}, \quad (2a)$$

$$\Pi = (\Pi_{\text{Re}} + i\Pi_{\text{Im}}) \begin{bmatrix} e^{i\psi} \sin(\theta/2) \\ e^{i(\psi+\phi)} \cos(\theta/2) \end{bmatrix}, \quad (2b)$$

where $\alpha, \beta, a, \Omega, b, \Pi_{\text{Re}}$, and Π_{Im} are real functions of t and ρ only. This ansatz has $\text{SU}(2)$ rather than $\text{U}(1) \times \text{U}(1)$

symmetry due to the equal rotation in the ψ and $\psi + \phi$ angles in orthogonal planes. This symmetry is preserved by Π . Without the scalar field, one finds that horizonless solutions have $\Omega = 0$ and, hence, do not rotate.

Gauge freedom is fixed by maximal slicing, where the trace of the extrinsic curvature $K = 0$ [79]. Unlike the choice $\beta = 0$ in other studies, this gauge allows for evolution beyond the formation of an apparent horizon.

In first-order form, our equations of motion contain 15 variables. Seven of these variables, namely, $\varphi_b, \varphi_r, \varphi_i, u_\beta, u_a, v_a$, and v_Ω , are defined by removing known boundary behavior from $b, \Pi_{\text{Re}}, \Pi_{\text{Im}}, \beta, a, \alpha$, and Ω , respectively. The remaining eight variables, $q_b, q_r, q_i, p_b, p_r, p_i, u_w$, and v_δ , are first-order variables. Henceforth, we may drop subscripts to represent vectors (each of rank 3), so that $\{\varphi, p, q, u, v\}$ contain our 15 dynamical functions. p and q are related to ρ and t derivatives of φ as

$$(1 - \rho^2) \partial_\rho \varphi + A^{(q)} \varphi = \frac{2}{\sqrt{a}} q, \quad (3a)$$

$$\partial_t \varphi = A^{(p)} p + B^{(p)} q + C^{(p)} \varphi, \quad (3b)$$

where the A s, B s, and C s are matrices containing expressions that may involve $\{u_\beta, u_a, v_a, v_\Omega, \rho\}$. u_w and v_δ are defined by

$$(1 - \rho^2) \partial_\rho v_a - 8\rho v_a + \frac{2\rho(1 - \rho^2)}{\sqrt{a}} v_\delta = F^{(\delta)}[\rho] u_a, \quad (4a)$$

$$(1 - \rho^2) \partial_\rho v_\Omega - 8\rho v_\Omega = F^{(w)}[\varphi_b, u_a, v_a] u_w, \quad (4b)$$

for some expressions $F^{(\delta)}$ and $F^{(w)}$.

The equations of motion, including the definitions above and the gauge condition $K = 0$, consists of 21 equations. With only 15 variables, six of the 21 equations are not solved directly and used only for initial data, postexcision boundary conditions, and numerical checks. These equations are (3a), and evolution equations for u ,

$$\partial_t u = f_u, \quad (5)$$

where f_u can depend on all the variables.

The 15 equations we solve directly can be expressed as a set of nine evolution equations and six nondynamical equations (i.e., equations without time derivatives). The evolution equations take the advection form

$$\begin{bmatrix} \partial_t \varphi \\ \partial_t q \\ \partial_t p \end{bmatrix} = \begin{bmatrix} 0 & 0 & 0 \\ \gamma A_\gamma & A_d & A_q \\ 0 & A_p & A_d \end{bmatrix} \begin{bmatrix} \partial_\rho \varphi \\ \partial_\rho q \\ \partial_\rho p \end{bmatrix} + \begin{bmatrix} f_\varphi \\ f_q + \gamma f_\gamma \\ f_p \end{bmatrix}, \quad (6)$$

where the A s are matrices that do not depend on φ, q , or p , and the f s are vectors that can depend on all variables. We have incorporated (3a) into these equations as damping terms with γ acting as a damping coefficient.

The six nondynamical equations take the form

$$A_u[\rho]\partial_\rho u + B_u[\rho, \varphi, p]u = g_u[\rho, \varphi, q, p, u], \quad (7a)$$

$$A_v[\rho]\partial_\rho v + B_v[\rho, \varphi, q, p, u]v = g_v[\rho, \varphi, q, p, u, v], \quad (7b)$$

where A_s and B_s are matrices and the g_s are vectors. Though (7) is a nonlinear system, given φ , q , and p , one can find u and v by solving a sequence of linear problems (see Supplemental Material for details [74]).

Initial data is supplied as a choice of φ and p . The remaining functions can be obtained by solving the nonlinear system (3a) and (7) using Newton-Raphson iteration. We evolve the system with a fourth-order Runge-Kutta method. At each step, φ , p , and q are evolved through (6), and u and v are obtained by solving (7) as a sequence of linear problems. We compute expansion coefficients from the metric to determine if a horizon has formed. We also monitor (5) and (3a) as a check on numerics.

At infinity ($\rho = 1$), we fix the boundary metric to be that of global AdS space and require $\Pi = 0$. The energy E and angular momentum J are read from the metric at infinity, and are conserved by (5). The response of the scalar field $\langle \Pi \rangle$ is obtained by

$$\Pi = (1 - \rho^2)^4 \langle \Pi \rangle + O((1 - \rho^2)^5). \quad (8)$$

Prior to horizon formation, we require regularity at the origin $\rho = 0$. After horizon formation, most points inside the horizon are excised, and boundary conditions at the excision surface are supplied for u through (5), and the value of v_δ is held fixed [80].

We use a spectral element mesh with Legendre-Gauss-Lobatto nodes, and interelement coupling handled by a discontinuous Galerkin method with Lax-Friedrichs flux. Adaptive mesh refinement for splitting elements and increasing or decreasing polynomial order is decided by monitoring the Legendre spectrum within each element. Linear systems are solved via a multifrontal method. Data presented here violate relative energy, momentum, and (3a) to within or below 10^{-8} . See the Supplemental Material for more numerical checks [74].

Gaussian data.—Consider Gaussian initial data

$$\Pi_{\text{Im}}|_{t=0} = \epsilon \rho \sqrt{2 - \rho^2} (1 - \rho^2)^4 e^{-4[2(1-\rho^2)-1]^2}, \quad (9a)$$

$$\left. \frac{\partial_t \Pi_{\text{Re}}}{\alpha \sqrt{a}} \right|_{t=0} = 4\lambda \Pi_{\text{Im}}, \quad (9b)$$

with the other functions within φ and p vanishing. This data is parametrized by ϵ and λ . At fixed λ and small varying ϵ , we have $E \propto \epsilon^2$ and $J \propto E$. This is a natural choice since individual normal modes of AdS space that carry angular momentum also obey $J \propto E$ at small E . We take two families of initial data: one with fixed $\lambda = 0$ where $J = 0$, and another with $\lambda = 1$, where $J \approx 0.155E$.

Let us describe the stationary black holes that can serve as final states of gravitational collapse. These black holes must fall within the symmetry class of our ansatz and have the same conserved quantities as our initial data. For $\lambda = 0$, we have $J = 0$ so the only stationary black holes are Schwarzschild-Tangherlini solutions.

For $\lambda = 1$, there are two competing families of regular black hole solutions. Myers-Perry black holes have the most entropy where they exist, i.e., for $E > E_{\text{extr}} \approx 0.0691$. For all energies $E < E_{\text{extr}}$, hairy black holes have the most entropy (by being the only existing solution). We wish to verify that gravitational collapse for the $\lambda = 1$ family will eventually settle into one of these black holes in accordance with their respective energy ranges. This can be viewed as a test of cosmic censorship, since Myers-Perry would be superextremal for $E < E_{\text{extr}}$.

A hairy black hole can be distinguished from the Myers-Perry case by the presence of the scalar field. In Fig. 1, we show the evolution of the normed square of the scalar response $|\langle \Pi \rangle|^2$ for two cases. In the first case, $E \approx 0.0873 > E_{\text{extr}}$, so the Myers-Perry configuration is the preferred solution. Indeed, we find that the scalar field vanishes at late times.

In the second case, $E \approx 0.0560 < E_{\text{extr}}$, so the Myers-Perry black hole is superextremal, and we find that the scalar field approaches a constant nonzero value at late times, indicative of a hairy black hole. We have also matched this value to that of the expected final hairy black-hole solution, which was first obtained in [72].

In both cases, we have also matched the final entropy and angular frequency to their respective final stationary solutions [72]. In the subextremal case, we have matched quasinormal modes as well. (See Supplemental Material [74].)

Now we compare the time scale for horizon formation between the $\lambda = 0$ ($J = 0$) and $\lambda = 1$ ($J \approx 0.155E$) families of initial data. In Fig. 2, we show a log-log plot of the collapse time versus the energy. We see that at fixed energy, the initial data with nonzero angular momentum takes a longer time to collapse. However, the collapse times for both sets of initial data exhibit a power law that is consistent with a $t \sim 1/E$ scaling. We conclude that in this case, angular momentum increases the collapse time but does not affect the time scale.

Boson star data.—Boson stars within our ansatz have been constructed in [72], and can be found by setting the metric to be time independent and the scalar field to have a harmonically oscillating complex phase. They can be parametrized by their harmonic frequency ω . For small energies, ω is close to a normal mode frequency of AdS space. We focus on the lowest frequency mode with $\omega = 5$ near AdS space. For small energies, these particular boson stars have angular momentum $J \approx 0.2E$.

As one increases the energy of the boson star, ω decreases until a turning point is reached around $\omega \approx 4.35$, where E and J are both maximal. Boson stars

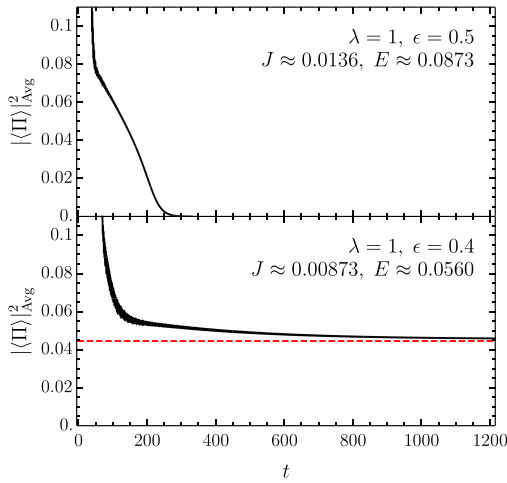


FIG. 1. Evolution of scalar response, averaged in a 2π time window, for Gaussian initial data. Top: Collapse occurs at $t \approx 30.1$ and settles to a Myers-Perry black hole. Bottom: Collapse occurs at $t \approx 55.4$ and settles to a hairy black hole. The red dashed line is the hairy black hole value from [72].

that lie on the AdS side of this turning point are expected to be nonlinearly stable (at least up to $t \sim 1/E$), and are otherwise expected to be unstable [81].

We perturb boson stars near the turning point with frequencies $\omega = 4.3$ (in the unstable branch) and $\omega = 4.4$ (in the stable branch) with a Gaussian profile similar to (9a). Their scalar response $|\langle \Pi \rangle|^2$ is shown in Fig. 3. Note that though the scalar field oscillates with frequency ω , these oscillations are canceled out in $|\Pi|^2$, and consequently are not seen in Fig. 3 nor in the metric.

Indeed, the $\omega = 4.3$ boson star is unstable, but the endpoint of its evolution depends on the perturbation. For one perturbation (top panel of Fig. 3), evolution proceeds rapidly towards gravitational collapse, and eventually settles to a Myers-Perry black hole. While a competing hairy black hole also exists, it has less entropy than Myers-Perry in this region of parameter space.

Perturbing the same boson star with the opposite sign yields drastically different results. As one can see from the middle panel of Fig. 3, large $O(1)$ deformations develop in

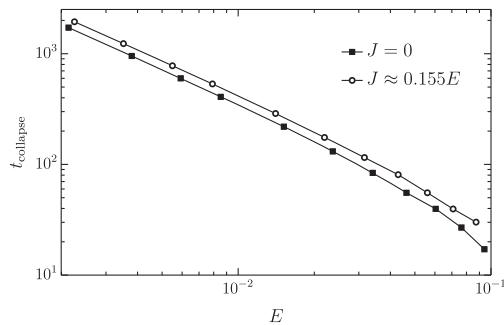


FIG. 2. Collapse times versus energy for Gaussian initial data. The power law is consistent with a $t \sim 1/E$ scaling. The two longest runs collapse at $t \approx 1721.12$ and $t \approx 1944.19$.

$|\langle \Pi \rangle|^2$ (and the metric) that oscillate for long times. The frequency of these oscillations is much smaller than the boson star frequency ω . The metric and scalar both oscillate, so the final state (assuming continued stability) might be characterized as an oscillon. Since the frequency ω is still present in the scalar, this solution is, in a sense, a multifrequency oscillon.

In contrast to the above, the lower panel of Fig. 3 shows that the perturbed boson with $\omega = 4.4$ remains stable at long times, with no large deviations from the initial data.

We have repeated this study for different perturbations and boson stars, and also for oscillons (where $\Pi_{\mathcal{I}} = 0$, see also [40]). We find no qualitative difference to the above.

Conclusions.—Our numerical results suggest that much of our understanding of the instability of AdS space carries over to situations with angular momenta as well. In particular, for generic data, the time scale for gravitational collapse $t \sim 1/E$ is preserved in the presence of rotation. Additionally, like oscillons in spherical symmetry, there are solutions that are nonlinear extensions of normal modes of AdS space that are stable past $t \sim 1/E$.

We have also found that, depending on the perturbation, unstable boson stars will either collapse or oscillate. A comparison can be made to situations in flat space where the endpoint of unstable solutions can also depend upon the perturbation (see, e.g., [73,82–86]). In flat space, energy and angular momentum can be carried away, and the noncollapsing evolution is well approximated by a perturbation of a stable boson star, presumably settling towards a stable boson star at asymptotically late time. By analogy, we suspect that the oscillating solution we find in AdS space can be described as a nonlinear extension of a perturbed stable boson star. In AdS space, however, there

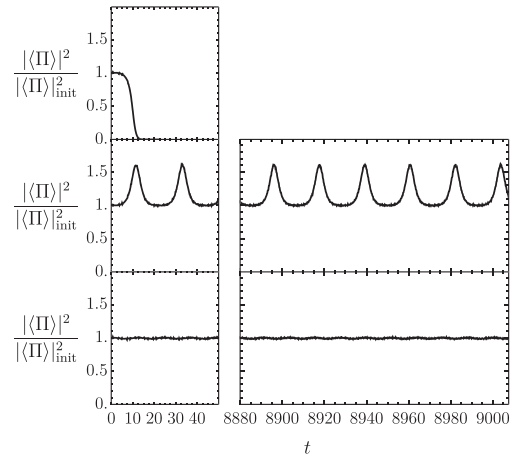


FIG. 3. Evolution of scalar response, scaled by its initial value, for perturbed boson stars near the turning point. Top: Boson star with $\omega = 4.3$ ($E \approx 0.392$) collapses into a Myers-Perry black hole. Middle: Boson star with $\omega = 4.3$ evolves to a stable oscillon. The perturbations for the top and middle plots differ by a sign. Bottom: Boson star with $\omega = 4.4$ ($E \approx 0.394$) remains stable.

is a reflecting boundary which may cause the oscillations to persist indefinitely.

Finally, let us comment on interesting regions of parameter space that we have not studied. There is a range of energies and angular momenta where hairy black holes have more entropy than Myers-Perry black holes. This happens to be where Myers-Perry black holes are unstable to superradiance. In fact, hairy black holes branch off from Myers-Perry configurations precisely at the onset of this instability, for particular perturbations [72].

This region is therefore a natural place to study the rotational superradiant instability [68,87–93], for which little is known fully dynamically. However, typical growth rates for this instability are around 10^{-5} [72], which requires a longer simulation than we can feasibly perform with our methods. Furthermore, our ansatz implies that such a study will necessarily be incomplete. High angular wave numbers are expected to play an important role in this instability [68,91–93], but our ansatz is restricted to only the $m = 1$ azimuthal wave numbers.

We would like to thank Mihalis Dafermos, Gary Horowitz, Luis Lehner, and Harvey Reall for reading an earlier version of the manuscript. The authors thankfully acknowledge the computer resources, technical expertise, and assistance provided by CENTRA/IST. Some computations were performed at the cluster “Baltasar-Sete-Sóis” and supported by the H2020 ERC Consolidator Grant “Matter and strong field gravity: New frontiers in Einstein’s theory,” Grant No. MaGRaTh-646597. Some computations were performed on the COSMOS Shared Memory system at DAMTP, University of Cambridge, operated on behalf of the STFC DiRAC HPC Facility and funded by BIS National E-infrastructure capital Grant No. ST/J005673/1 and STFC Grants No. ST/H008586/1 and No. ST/K00333X/1. O. J. C. D. is supported by the STFC Ernest Rutherford Grants No. ST/K005391/1 and No. ST/M004147/1. M. W. C. and B. W. are supported by NSERC.

*choptuik@physics.ubc.ca

†O.J.Campos-Dias@soton.ac.uk

*jss55@cam.ac.uk

§benson@phas.ubc.ca

- [1] J. M. Maldacena, *Int. J. Theor. Phys.* **38**, 1113 (1999).
- [2] S. S. Gubser, I. R. Klebanov, and A. M. Polyakov, *Phys. Lett. B* **428**, 105 (1998).
- [3] E. Witten, *Adv. Theor. Math. Phys.* **2**, 253 (1998).
- [4] O. Aharony, S. S. Gubser, J. M. Maldacena, H. Ooguri, and Y. Oz, *Phys. Rep.* **323**, 183 (2000).
- [5] M. Dafermos and G. Holzegel, Dynamic instability of solitons in $4 + 1$ dimensional gravity with negative cosmological constant, in Seminar at DAMTP, Cambridge, England, 2006, <https://www.dpmms.cam.ac.uk/~md384/ADSinstability.pdf>.
- [6] M. Dafermos, The problem of stability for black hole spacetimes, in Newton Institute, Cambridge, England,

- 2006, <http://www-old.newton.ac.uk/webseminars/pg+ws/2006/gmx/1010/dafermos/>.
- [7] H. Friedrich, *J. Geom. Phys.* **3**, 101 (1986).
- [8] D. Christodoulou and S. Klainerman, *The Global Nonlinear Stability of the Minkowski Space* (Princeton University Press, Princeton, NJ, 1993).
- [9] P. Bizon and A. Rostworowski, *Phys. Rev. Lett.* **107**, 031102 (2011).
- [10] O. J. C. Dias, G. T. Horowitz, and J. E. Santos, *Classical Quantum Gravity* **29**, 194002 (2012).
- [11] O. J. C. Dias, G. T. Horowitz, D. Marolf, and J. E. Santos, *Classical Quantum Gravity* **29**, 235019 (2012).
- [12] A. Buchel, L. Lehner, and S. L. Liebling, *Phys. Rev. D* **86**, 123011 (2012).
- [13] A. Buchel, S. L. Liebling, and L. Lehner, *Phys. Rev. D* **87**, 123006 (2013).
- [14] M. Maliborski and A. Rostworowski, *Phys. Rev. Lett.* **111**, 051102 (2013).
- [15] P. Bizon and J. Jał mużna, *Phys. Rev. Lett.* **111**, 041102 (2013).
- [16] M. Maliborski, *Phys. Rev. Lett.* **109**, 221101 (2012).
- [17] M. Maliborski and A. Rostworowski, [arXiv:1307.2875](https://arxiv.org/abs/1307.2875).
- [18] R. Baier, S. A. Stricker, and O. Taanila, *Classical Quantum Gravity* **31**, 025007 (2014).
- [19] J. Jał mużna, *Acta Phys. Pol. B* **44**, 2603 (2013).
- [20] P. Basu, D. Das, S. R. Das, and T. Nishioka, *J. High Energy Phys.* **03** (2013) 146.
- [21] O. Gannot, *Commun. Math. Phys.* **330**, 771 (2014).
- [22] G. Fodor, P. Forgács, and P. Grandclément, *Phys. Rev. D* **89**, 065027 (2014).
- [23] H. Friedrich, *Classical Quantum Gravity* **31**, 105001 (2014).
- [24] P. Bizon and A. Rostworowski, *Acta Phys. Pol., B* **48**, 1375 (2017).
- [25] M. Maliborski and A. Rostworowski, *Phys. Rev. D* **89**, 124006 (2014).
- [26] J. Abajo-Arastia, E. da Silva, E. Lopez, J. Mas, and A. Serantes, *J. High Energy Phys.* **05** (2014) 126.
- [27] V. Balasubramanian, A. Buchel, S. R. Green, L. Lehner, and S. L. Liebling, *Phys. Rev. Lett.* **113**, 071601 (2014).
- [28] P. Bizon and A. Rostworowski, *Phys. Rev. Lett.* **115**, 049101 (2015).
- [29] V. Balasubramanian, A. Buchel, S. R. Green, L. Lehner, and S. L. Liebling, *Phys. Rev. Lett.* **115**, 049102 (2015).
- [30] E. da Silva, E. Lopez, J. Mas, and A. Serantes, *J. High Energy Phys.* **04** (2015) 038.
- [31] B. Craps, O. Evnin, and J. Vanhoof, *J. High Energy Phys.* **10** (2014) 048.
- [32] P. Basu, C. Krishnan, and A. Saurabh, *Int. J. Mod. Phys. A* **30**, 1550128 (2015).
- [33] N. Deppe, A. Kolly, A. Frey, and G. Kunstatter, *Phys. Rev. Lett.* **114**, 071102 (2015).
- [34] F. V. Dimitrakopoulos, B. Freivogel, M. Lippert, and I.-S. Yang, *J. High Energy Phys.* **08** (2015) 077.
- [35] G. T. Horowitz and J. E. Santos, *Surv. Differ. Geom.* **20**, 321 (2015).
- [36] A. Buchel, S. R. Green, L. Lehner, and S. L. Liebling, *Phys. Rev. D* **91**, 064026 (2015).
- [37] B. Craps, O. Evnin, and J. Vanhoof, *J. High Energy Phys.* **01** (2015) 108.

- [38] P. Basu, C. Krishnan, and P. N. Bala Subramanian, *Phys. Lett. B* **746**, 261 (2015).
- [39] I.-S. Yang, *Phys. Rev. D* **91**, 065011 (2015).
- [40] G. Fodor, P. Forgács, and P. Grandclément, *Phys. Rev. D* **92**, 025036 (2015).
- [41] H. Okawa, J. C. Lopes, and V. Cardoso, [arXiv:1504.05203](https://arxiv.org/abs/1504.05203).
- [42] P. Bizon, M. Maliborski, and A. Rostworowski, *Phys. Rev. Lett.* **115**, 081103 (2015).
- [43] F. Dimitrakopoulos and I.-S. Yang, *Phys. Rev. D* **92**, 083013 (2015).
- [44] S. R. Green, A. Maillard, L. Lehner, and S. L. Liebling, *Phys. Rev. D* **92**, 084001 (2015).
- [45] N. Deppe and A. R. Frey, *J. High Energy Phys.* **12** (2015) 004.
- [46] B. Craps, O. Evnin, and J. Vanhoof, *J. High Energy Phys.* **10** (2015) 079.
- [47] B. Craps, O. Evnin, P. Jai-akson, and J. Vanhoof, *J. High Energy Phys.* **10** (2015) 080.
- [48] O. Evnin and C. Krishnan, *Phys. Rev. D* **91**, 126010 (2015).
- [49] D. S. Menon and V. Suneeta, *Phys. Rev. D* **93**, 024044 (2016).
- [50] J. Jalmuzna, C. Gundlach, and T. Chmaj, *Phys. Rev. D* **92**, 124044 (2015).
- [51] O. Evnin and R. Nivesvivat, *J. High Energy Phys.* **01** (2016) 151.
- [52] B. Freivogel and I.-S. Yang, *Phys. Rev. D* **93**, 103007 (2016).
- [53] O. Dias and J. E. Santos, *Classical Quantum Gravity* **33**, 23LT01 (2016).
- [54] O. Evnin and P. Jai-akson, *J. High Energy Phys.* **04** (2016) 054.
- [55] N. Deppe, [arXiv:1606.02712](https://arxiv.org/abs/1606.02712).
- [56] F. V. Dimitrakopoulos, B. Freivogel, J. F. Pedraza, and I.-S. Yang, *Phys. Rev. D* **94**, 124008 (2016).
- [57] F. V. Dimitrakopoulos, B. Freivogel, and J. F. Pedraza, [arXiv:1612.04758](https://arxiv.org/abs/1612.04758).
- [58] A. Rostworowski, *Classical Quantum Gravity* **34**, 128001 (2017).
- [59] J. Jalmuzna and C. Gundlach, *Phys. Rev. D* **95**, 084001 (2017).
- [60] A. Rostworowski, *Phys. Rev. D* **95**, 124043 (2017).
- [61] G. Martinon, G. Fodor, P. Grandclément, and P. Forgács, *Classical Quantum Gravity* **34**, 125012 (2017).
- [62] G. Moschidis, [arXiv:1704.08685](https://arxiv.org/abs/1704.08685).
- [63] G. Moschidis, [arXiv:1704.08681](https://arxiv.org/abs/1704.08681).
- [64] O. J. C. Dias and J. E. Santos, [arXiv:1705.03065](https://arxiv.org/abs/1705.03065).
- [65] P. Bizon, *Gen. Relativ. Gravit.* **46**, 1724 (2014).
- [66] M. Maliborski and A. Rostworowski, *Int. J. Mod. Phys. A* **28**, 1340020 (2013).
- [67] B. Craps and O. Evnin, *Fortschr. Phys.* **64**, 336 (2016).
- [68] O. J. C. Dias, J. E. Santos, and B. Way, *J. High Energy Phys.* **12** (2015) 171.
- [69] H. Bantilan, P. Figueras, M. Kunesch, and P. Romatschke, preceding Letter, *Phys. Rev. Lett.* **119**, 191103 (2017).
- [70] P. Bizon, T. Chmaj, and B. G. Schmidt, *Phys. Rev. Lett.* **95**, 071102 (2005).
- [71] P. Bizon, T. Chmaj, G. W. Gibbons, C. N. Pope, *Classical Quantum Gravity* **24**, 4751 (2007).
- [72] O. J. C. Dias, G. T. Horowitz, and J. E. Santos, *J. High Energy Phys.* **07** (2011) 115.
- [73] S. L. Liebling and C. Palenzuela, *Living Rev. Relativ.* **15**, 6 (2012).
- [74] See Supplemental Material at <http://link.aps.org/supplemental/10.1103/PhysRevLett.119.191104> for details on the equations of motion, numerical validation, the matching of final states to stationary solutions, and the linear perturbation of boson stars.
- [75] V. Balasubramanian and P. Kraus, *Commun. Math. Phys.* **208**, 413 (1999).
- [76] S. de Haro, S. N. Solodukhin, and K. Skenderis, *Commun. Math. Phys.* **217**, 595 (2001).
- [77] O. J. C. Dias, J. E. Santos, and B. Way, *Classical Quantum Gravity* **33**, 133001 (2016).
- [78] P. Figueras, K. Murata, and H. S. Reall, *J. High Energy Phys.* **11** (2012) 071.
- [79] M. W. Choptuik, E. W. Hirschmann, and R. L. Marsa, *Phys. Rev. D* **60**, 124011 (1999).
- [80] A choice of v_δ at the excision surface fixes residual gauge freedom.
- [81] Morse theory typically implies that solutions on one side of a turning point are unstable. For completeness, we demonstrate linear instability in the Supplemental Material [74].
- [82] T. D. Lee and Y. Pang, *Nucl. Phys.* **B315**, 477 (1989).
- [83] E. Seidel and W.-M. Suen, *Phys. Rev. D* **42**, 384 (1990).
- [84] C. W. Lai and M. W. Choptuik, [arXiv:0709.0324](https://arxiv.org/abs/0709.0324).
- [85] N. Sanchis-Gual, C. Herdeiro, E. Radu, J. C. Degollado, and J. A. Font, *Phys. Rev. D* **95**, 104028 (2017).
- [86] P. Carracedo, J. Mas, D. Musso, and A. Serantes, *J. High Energy Phys.* **05** (2017) 141.
- [87] S. W. Hawking and H. S. Reall, *Phys. Rev. D* **61**, 024014 (1999).
- [88] V. Cardoso and O. J. C. Dias, *Phys. Rev. D* **70**, 084011 (2004).
- [89] H. K. Kunduri, J. Lucietti, and H. S. Reall, *Phys. Rev. D* **74**, 084021 (2006).
- [90] O. J. C. Dias and J. E. Santos, *J. High Energy Phys.* **10** (2013) 156.
- [91] V. Cardoso, O. J. C. Dias, G. S. Hartnett, L. Lehner, and J. E. Santos, *J. High Energy Phys.* **04** (2014) 183.
- [92] B. E. Niehoff, J. E. Santos, and B. Way, *Classical Quantum Gravity* **33**, 185012 (2016).
- [93] S. R. Green, S. Hollands, A. Ishibashi, and R. M. Wald, *Classical Quantum Gravity* **33**, 125022 (2016).